

# Seeing the Fields and Forests: Application of Surface-Layer Theory and Flux-Tower Data to Calculating Vegetation Canopy Height

Sam Pennypacker<sup>1</sup> · Dennis Baldocchi<sup>2</sup>

Received: 22 December 2014 / Accepted: 10 September 2015 / Published online: 29 September 2015  
© Springer Science+Business Media Dordrecht 2015

**Abstract** Canopy height is an important and dynamic site variable that affects the mass and energy exchanges between vegetation and the atmosphere. We develop a method to estimate canopy height routinely, using surface-layer theory and turbulence measurements made from a collection of flux towers. This tool is based on connecting the logarithmic wind profile generally expected in a neutral surface layer with direct measurements of friction velocity and assumptions about canopy height's relationships with zero-plane displacement and aerodynamic roughness length. Tests over a broad range of canopy types and heights find that calculated values are in good agreement with direct measurements of canopy height, including in a heterogeneous landscape. Based on the various uncertainties associated with our starting assumptions about canopy micrometeorology, we present a blueprint for future work that is necessary for expanding and improving these initial calculations.

**Keywords** Canopy height · Eddy covariance · Lidar verification · Surface-layer theory

## 1 Introduction

Canopy height is an important attribute of a landscape that affects surface roughness and thus wind profiles that relate to momentum transfer in the lower atmosphere (Shaw and Pereira 1982). It also affects vegetation albedo (Dickinson and Hanson 1984; Ni and Woodcock 2000) and scales with above-ground biomass (Lefsky et al. 2002; Drake et al. 2003; Lefsky et al. 2005; Thomas et al. 2008). Lidar techniques have been used extensively in the past

---

✉ Sam Pennypacker  
spennypacker@berkeley.edu

Dennis Baldocchi  
baldocchi@berkeley.edu

<sup>1</sup> Department of Earth and Planetary Science, University of California, Berkeley, Berkeley, CA 94720, USA

<sup>2</sup> Department of Environmental Science, Policy and Management, University of California, Berkeley, Berkeley, CA 94720, USA

decade to measure forest canopy height from space (Lefsky et al. 2005; Simard et al. 2011), from aircraft (Chen and Hay 2011; Saremi et al. 2014) and from ground-based instruments (Lovell et al. 2003).

These methods require validation, however, because of uncertainties arising from spatial resolution limits and variations in vegetation density and landscape topography (Mascaro et al. 2011; Saremi et al. 2014). Additionally, vegetation height is an important metric of crop response to climate change and can be used to estimate components of the water balance in agricultural regions (Devkota et al. 2013; Timm et al. 2014). Traditionally, canopy height is determined manually either with rough estimates by eye or using devices such as hypsometers. Additionally, field campaigns are labour and resource intensive and cannot provide a continuous, long-term record of growth and change needed to apply knowledge of canopy height in these kinds of studies. Given the importance of canopy height's relation to biosphere-atmosphere interactions, it is necessary to develop quantitatively rigorous techniques that can be applied cheaply using data available in a variety of climates and ecosystems. This will allow for independent and accessible calculations of canopy height that can be used to support lidar campaigns and the improvement of canopy models.

The advent of a global network of eddy-covariance towers has provided invaluable data on turbulence in and around vegetation canopies worldwide. These data are critical for quantifying fluxes between the atmosphere and biosphere, and we use them to develop and test a method for calculating vegetation canopy height based on surface-layer theory. Section 3 presents time series and distributions of calculated canopy heights from short crops to tall forest canopies; we then test the sensitivity of our method to different components of a heterogeneous canopy with varying wind direction and flux footprints. This is important for improving estimates of canopy height in multi-species landscapes and determining the impact of flux footprints on comparing calculated canopy height to lidar measurements. Section 4 includes discussion of the steps needed to improve upon this initial work given the uncertainties associated with flux-tower measurements and filtering methodology. Wherever possible, we compare estimates of canopy height taken from external sources to our calculations.

## 2 Methods

### 2.1 Theory

The foundation of our method is an application of the logarithmic wind profile based on Monin–Obukhov similarity theory for a neutral surface layer (Garratt 1994). The equation in gradient and integrated forms are shown below for reference, where  $u$  is the horizontal wind speed at height  $z$ ,  $u_*$  is the friction velocity,  $k = 0.4$  is the von Karman constant,  $z_0$  is the aerodynamic roughness length and  $d$  is the zero-plane displacement.

$$\left(\frac{z-d}{u_*}\right) \frac{\partial u}{\partial z} = \frac{1}{k}, \quad (1)$$

$$u(z) = \left(\frac{u_*}{k}\right) \ln\left(\frac{z-d}{z_0}\right). \quad (2)$$

A variety of observational work done to characterize the spectra of turbulence inside and immediately above rough canopies has shown that this classic surface-layer formulation fails close to the top of a canopy (Finnigan 2000). High shear at the vegetation–atmosphere interface leads to wind profiles and turbulence statistics that are not predicted by Monin–

Obukhov similarity theory inside the roughness sublayer (Raupach et al. 1996). The depth of this roughness sublayer, and thus the depth over which wind speed diverges from Eq. 2, is not completely constrained, but it has been estimated to extend no further than twice the canopy height (Finnigan 2000). We assess parameters of the wind profile based on wind speed and friction velocity measurements made near and above the edge of the roughness sublayer by this definition. At these heights, we assume it is reasonable to extrapolate the effects of the canopy onto a logarithmic profile.

In order to connect Eq. 2 to vegetation canopy height ( $h$ ), we rely on estimates of the ratios  $d/h$  and  $z_0/h$  developed by Raupach (1994) for use in numerical climate models. These parametrizations are functions of leaf area index (LAI), but we start with the typical values  $d/h = 0.6$  and  $z_0/h = 0.1$ , and include an analysis of the validity of these assumptions in the later discussion. Thus, we obtain an analytical equation for canopy height that uses variables measured at most flux-tower sites,

$$h = \frac{z}{0.6 + 0.1 \exp\left(\frac{ku}{u_*}\right)}. \quad (3)$$

## 2.2 Flux Measurements

All data are obtained from the eddy-covariance towers discussed below. Towers are equipped with three-dimensional sonic anemometers for continuous, high frequency measurements of the three wind velocity components ( $u$ ,  $v$  and  $w$ ) and typically have infrared gas analyzers to measure water vapour and CO<sub>2</sub> concentrations. The wind velocities are divided into a mean flow component ( $\bar{u}$ ,  $\bar{v}$  and  $\bar{w}$ ) and a fluctuation component ( $u'$ ,  $v'$  and  $w'$ ). One of the most important measurements needed for Eq. 3,  $u_*$ , is defined in terms of the air density  $\rho$  and Reynolds shear stress  $\tau$ ,

$$u_*^2 = \frac{\tau}{\rho} = \left| \overline{u'w'} \right|. \quad (4)$$

The sensible heat flux ( $H$ ) is calculated using  $\rho$ , the specific heat capacity of air ( $c_p$ ), and the covariance of acoustic virtual temperature fluctuations  $T'$  and fluctuations in vertical wind speed  $w'$ ,

$$H = \rho c_p \overline{w'T'}. \quad (5)$$

Acoustic virtual temperature is calculated using wind speeds measured by the sonic anemometer and their relationship to the speed of sound. This eliminates the need for thermocouples that can be easily broken and contribute error to measurements through their thermal inertia. Generally, data are collected at 10–50 Hz and are reported on 30-min blocks.

## 2.3 Filtering

We first consider the static stability of the air surrounding the tower since Eq. 2 is only valid in neutral conditions (Garratt 1994). We use the non-dimensional Obukhov length ( $z/L$ ) as the metric to define stability for each timestep that data are reported by the eddy-covariance system,

$$\frac{z}{L} = -\frac{zkgH}{u_*^3\theta\rho c_p}, \quad (6)$$

where  $g$  is the acceleration due to gravity and  $\theta$  is potential temperature, and when  $z/L$  approaches zero the atmosphere is neutrally buoyant. Monin–Obukhov similarity theory

holds that non-dimensional descriptions of wind profiles in the surface layer (e.g., Eq. 1) can be expressed as a function ( $\phi_M$ ) of  $z/L$  alone (Garratt 1994). In neutral conditions  $\phi_M = 1$ , and Eq. 1 is recovered. Establishing the acceptable threshold for near-neutral conditions is crucial, and we use  $\phi_M$  to diagnose the impact of various cut-offs on the validity of applying the logarithmic profile. We consider a balance between being close to near-neutral conditions while maintaining a large enough sample size ( $N$ ) to calculate robust daily averages to be very important. Both deviations from a logarithmic profile and inadequate values of  $N$  (daily and yearly) can contribute errors in our canopy height calculations, and it is important to determine which is most affected by the filtering criteria.

A variety of other work over the past several decades has defined near-neutral conditions when  $|z/L| \lesssim 0.1$  for practical purposes (Hogstrom 1988; Oncley et al. 1996; Marcolla et al. 2005; Draxl et al. 2012). This assumption has been tested at field sites by comparing the logarithmic profile with observed wind profiles (Peña et al. 2014) and verifying that buoyancy effects are in fact reduced by an order of magnitude with this condition for near-neutrality (Metzger et al. 2007). We further test whether  $|z/L| < 0.1$  is sufficient for our analysis by considering the effects of setting the threshold for  $|z/L|$  at 0.03 and 0.1 on  $\phi_M$  and total sample size at our study sites. Wind-profile observations have suggested that  $\phi_M$  can be written as

$$\phi_M = \left(1 - \gamma_1 \left(\frac{z}{L}\right)\right)^{-1/4}, \quad (7)$$

$$\phi_M = 1 + \beta_1 \left(\frac{z}{L}\right), \quad (8)$$

in unstable ( $-5 < z/L < 0$ ) and stable ( $0 < z/L < 1$ ) conditions, with the empirical parameters  $\gamma_1$  and  $\beta_1$  taken to be 16 and 5, respectively (Dyer 1974; Garratt 1994). Initial calculations indicate that the mean, median and mode wind profiles at all of our sites sit close to logarithmic as  $\phi_M = 1$  to within about 5% on yearly time scales. Applying the more stringent requirement that  $|z/L| < 0.03$  reduces the sample size by between 40 and 65% for the time windows over which we calculate canopy height at each site. However, the mean, median and mode of values of  $\phi_M$  differ by a few percent when the different filters are applied; using  $|z/L| < 0.03$  brings the mean, median and mode wind profiles at each site only slightly closer to logarithmic. At one standard deviation from the average  $z/L$ ,  $\phi_M$  deviates from its neutral value by between 20 and 40% when using the  $|z/L| < 0.1$  threshold and by about 10% when using  $|z/L| < 0.03$ , depending on the site. Since the  $z/L$  threshold has a larger relative impact on the available sample size than the statistics of  $\phi_M$ , we elect to exclude data when  $|z/L| > 0.1$  in order to optimize the reduction in error. We will return to the validity and importance of this decision in the later discussion.

We also apply friction velocity thresholds to ensure there is enough turbulence for eddy covariance. Minimum friction velocity filters have been established by analysis of nighttime CO<sub>2</sub> flux data (Gu et al. 2005). These thresholds have often been determined by visual inspection, though a more thorough analysis revealed that on average a minimum  $u_* = 0.2 \text{ m s}^{-1}$  is important for robust eddy-covariance measurements (Papale et al. 2006). This average was determined using scalar data from 12 flux tower sites, and while there is important site-to-site variability, we will use the average as our minimum threshold. We also implement an upper bound on  $u_*$  in order to avoid extreme canopy conditions, as well. We want to be cautious about using too high of  $u_*$  values as they may cause deformation in the canopy, as when plants bend over or experience waves and honami (Finnigan 1979; Gardiner 1994). The upper bounds for the rice ( $0.4 \text{ m s}^{-1}$ ), alfalfa site ( $0.4 \text{ m s}^{-1}$ ), citrus grove ( $0.5 \text{ m s}^{-1}$ ), evergreen broadleaf ( $0.8 \text{ m s}^{-1}$ ), evergreen conifer ( $0.6 \text{ m s}^{-1}$ ) and oak savannah ( $0.5 \text{ m s}^{-1}$ )

sites are all one standard deviation from the average  $u_*$  value at that site. Since we are trying to invert canopy structure from turbulence measurements we do not need data from all wind conditions, just the best ones. The stability and  $u_*$  thresholds give us a range of conditions over which to estimate canopy height, and could be adjusted for future work. At the rice site, we also only consider data from wind directions that passed over the vegetation of interest due to the orientation of the tower with respect to the field.

## 2.4 Site Selection and Validation Measurements

Sites are selected in order to capture a full range of vegetation types and heights. We begin with short crops, rice and alfalfa, in the Sacramento–San Joaquin Delta of California (Knox et al. 2014). We then move on to a citrus grove of intermediate height in Southern California (Fares et al. 2012). We also use two evergreen forests that are part of the global FLUXNET system, one in Washington State, USA (conifer evergreen) and one in Australia (broadleaf evergreen) for the tall end of the height spectrum (Paw et al. 2004; Parker et al. 2004; Leuning et al. 2005). These sites have been extensively studied with lidar and are thus ideal for testing our method's ability to serve as a lidar verification tool (Kane et al. 2010; Hopkinson et al. 2013). These studies provide a range of canopy height estimates used for verification, though we focus on the average values since we are also calculating averages. Finally, we present results from an oak savannah in Northern California, also managed by the Berkeley Biometeorology Group, as an example of a heterogeneous canopy (Ma et al. 2007). Table 1 summarizes important geographic and background information for each site.

## 2.5 Data Representation and Statistical Comparison to Reference Values

Results are separated into seasonal crops (rice and alfalfa), and non-seasonal trees, the citrus grove, broadleaf (Tumbarumba), conifer (Wind River) and oak savannah (Tonzi). This separation was motivated by the difference in the kinds of applications best suited for each site. For the crop sites, we present time series of calculated daily average height. A daily average is appropriate because canopy height does not measurably change between 30-min eddy-covariance timesteps. Furthermore, considering a larger sample size reduces the impact of random error in calculating average canopy height (Moncrieff et al. 1996). For the tree-dominated sites, we create distributions of the daily-averaged calculated canopy height. These canopies do not experience the same kind of seasonal growth cycle as the rice and alfalfa. The probability distributions allow for the analysis of a range of statistics for a given year or over multiple years. At the heterogeneous savannah site, we calculate height statistics in each Cartesian quadrant around the tower.

In order to quantitatively assess the accuracy of our calculations, we compute the mean absolute error (*MAE*) of a one-to-one comparison between the calculated heights and previously estimated reference heights,

$$MAE = \sum \frac{|h_{\text{model}} - h_{\text{calc}}|}{N}, \quad (9)$$

where  $h_{\text{calc}}$  is the calculated height, and  $h_{\text{model}}$  is the predicted value of  $h$ , taken to be the previous estimate. The value of *MAE* is a measure of the average error for a particular model, which is a one-to-one line between calculated and reference heights in the present study. For the crops, we compare the measured daily averages against daily average calculations and for the forest sites we compare estimated and calculated yearly averages. We can also calculate

**Table 1** Summary of sites used for this study

Site name	Latitude	Longitude	Elevation (m)	Dominant vegetation type	Tower height (z; m)	Independent validation measurements
Rice	38.1055N	121.6521W	-9	Rice	3.25	By hand in growing season
Alfalfa	38.1159N	121.6467W	-9	Alfalfa	2.8	By hand in growing season
Tumbarumba	-35.6557S	148.1521E	932	Broadleaf evergreen	70	Mean: 40 m
Wind River	45.8205N	121.9519W	371	Conifer evergreen	74.5	Mean: 56.3 m
Tonzi Ranch	38.4316N	120.9660W	169	Oak savannah	23	Mean: 9.4 m
Citrus Grove	36.3566N	119.09226W	131	Orange trees	7.11 & 9.18	4.2 ± 0.2 m

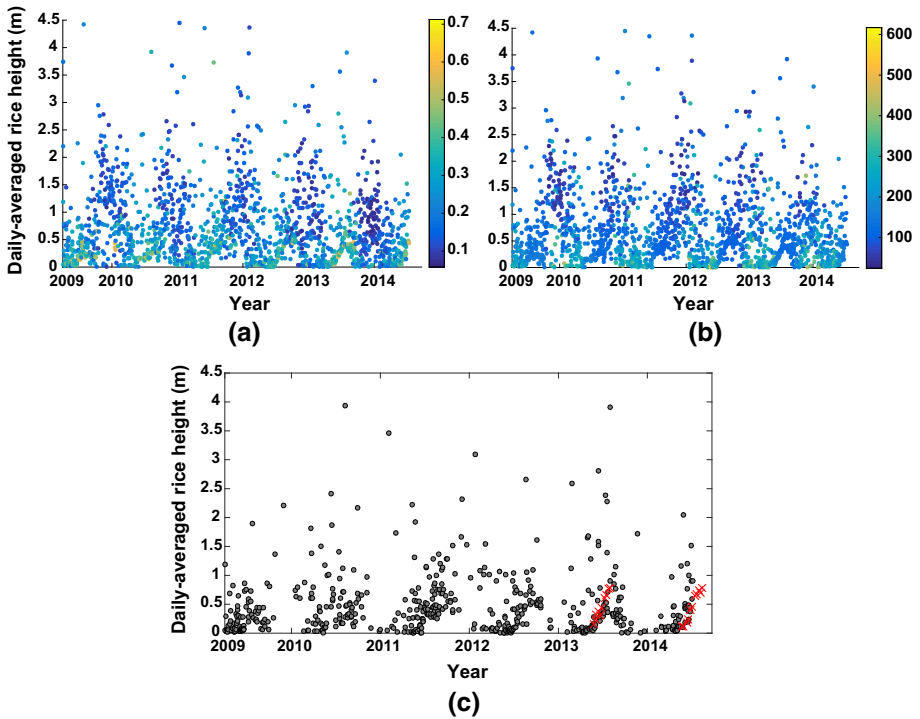


**Fig. 1** **a** Daily-averaged rice height with stability filter applied and friction velocity *colour bar*, **b** daily-averaged rice height with stability filter applied and drag coefficient *colour bar*, **c** daily-averaged rice height with all filters

the so-called mean bias error (Willmott and Matsuura 2005), which indicates whether the calculated canopy heights tend to be less than or greater than the previous estimates,

$$MBE = \sum \frac{h_{\text{model}} - h_{\text{calc}}}{N}. \tag{10}$$

If  $MBE > 0$ , our daily average calculations tend to be smaller than the previously estimated reference values. These statistics allow for comparison across a variety of canopy types and provide quantitative information about the performance of calculated values against other estimates of canopy height.

### 3 Results

#### 3.1 Rice and Alfalfa (Short Height)

We first use data for the rice site over five years of growing seasons. Concurrent field data are marked in red in Fig. 1c along with our calculations. Figure 1a, b show height calculations with corresponding daily average friction velocity and drag coefficient  $(u/u_*)^2$  in colour. The calculations capture a consistent pattern of seasonal growth, but there are outliers with heights up to approximately 5 m. Figure 1a highlights how critical the  $u_*$  filter is for obtaining the final results shown in Fig. 1c; the filtering clearly reduces the spread in our calculated

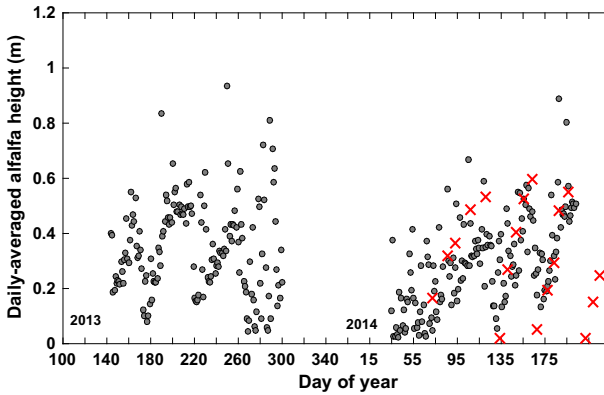


**Fig. 2** Daily-averaged alfalfa height during the growing seasons of 2013 and 2014 with average field measurements in red

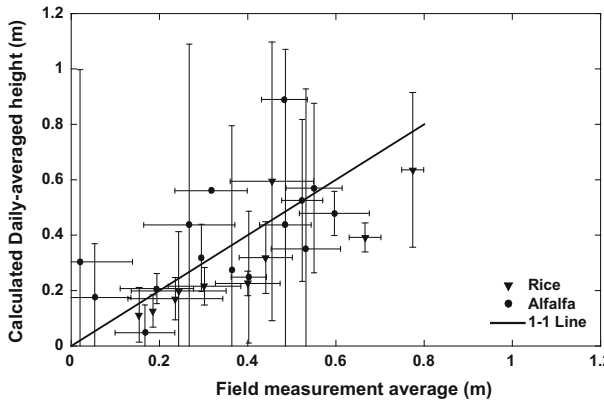


**Fig. 3** Measured versus calculated averages for both crop sites with a 1–1 line. Vertical error bars are one standard deviation around the daily average. Horizontal error bars are one standard deviation around average field measurements

estimates of rice height. Furthermore, we can use Fig. 1b to examine connections between the drag coefficient and outliers in calculated canopy height. Figure 2 shows daily-averaged heights calculated from two years of available data from the growing season at the alfalfa site. Field measurements are again included in red for comparison. The calculations clearly reflect the abrupt changes in height caused by periodic summer mowing and the subsequent regrowth shown by the field measurements. The alfalfa exhibits fewer outlier calculations than the rice, and we examine possible explanations in Sect. 4. Using days where field measurements are available, Fig. 3 shows how well the daily average calculations fall along a one-to-one line for both crop sites. The MAE value for the one-to-one line and the calculated averages is 0.087 and  $MBE = 0.008$ . In general, this indicates low error about the one-to-one line, with our calculated values tending to be slightly lower than field measurements.

### 3.2 Citrus Grove (Intermediate Height)

We now test our method with vegetation of intermediate height with one year of data (2010) from the citrus grove. The mean heights from 2010 are similar from both tower heights. However, the canopy height distributions from each tower height are not identical, as seen



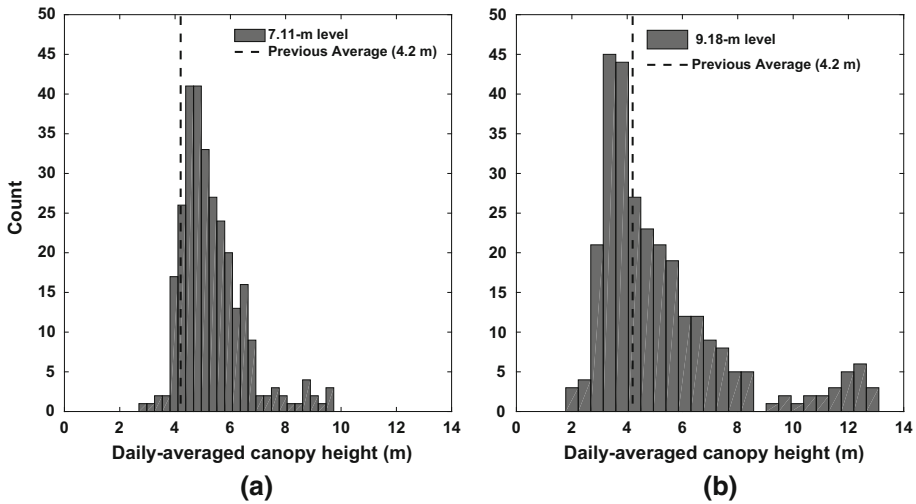


**Fig. 4** Distributions of calculated canopy height from **a** 7.11-m level and **b** 9.18-m level with previous averages for reference from [Fares et al. \(2012\)](#)

**Table 2** Yearly average, median and standard deviations for heights calculated at the two citrus grove tower levels

Tower level (m)	2010 yearly average (m)	2010 yearly standard deviation (m)	2010 yearly median (m)
7.11	5.3	1.2	5.1
9.18	5.2	2.0	4.4

in Fig. 4. This is also reflected in the statistics of Table 2. The calculations from the 9.18-m level measurements yielded a higher standard deviation than the 7.11-m level calculations. Figure 4a shows calculated daily average heights up to approximately 12 m from the higher tower level, and the wider distribution is likely biasing our average. On the other hand, the median height from the 9.18-m level data is closer in line with the previous estimate of  $4.2 \pm 0.2$  m ([Fares et al. 2012](#)).

### 3.3 Forest Canopies (Tall Height)

Figure 5 shows the distributions at a broadleaf evergreen (Tumbarumba) and conifer evergreen (Wind River) sites. Table 3 details the statistics for the years considered at both sites. The previously determined average estimates are all within 4 m ( $\approx 40\%$  of yearly standard deviations) of our calculations at the broadleaf evergreen and 7 m ( $\approx 70\%$  of yearly standard deviations). We also see that the standard deviation around our overall, multi-year average is small, indicating low inter-annual variability in our calculations. Small variations in meteorological conditions, flux footprint and canopy phenology are smoothed out of the yearly averages.

### 3.4 Heterogeneous Canopy

The heterogeneity of the oak-savannah (Tonzi) site is clear in the airborne lidar scan (Fig. 6) of the area taken in 2009 ([Chen et al. 2006](#); [Baldocchi et al. 2010](#)). Height roses with calculated canopy height binned by wind direction are shown in Fig. 7. Qualitatively, we see from the

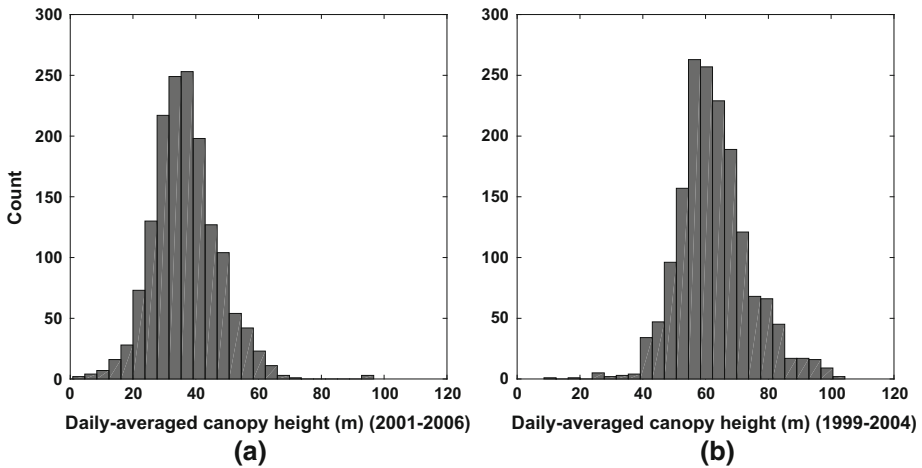


**Fig. 5** Distributions of daily-averaged canopy height at **a** broadleaf evergreen site and **b** conifer evergreen site

**Table 3** Statistics for multiple years at the forest sites for comparisons to previous estimates

Year (broadleaf)	Average calculated height (m)	SD	Year (conifer)	Average calculated height (m)	SD
2001	37.8	10.4	1999	63.6	10.6
2002	37.4	10.4	2000	60.9	11.8
2003	36.04	10.8	2001	62.6	11.9
2004	36.8	10.4	2002	63.2	12.9
2005	36.0	9.9	2004	62.3	9.2
2006	36.2	8.8			
Multi-year	36.7	0.75	Multi-year	62.6	0.94

Previous estimate of broadleaf average is 40 m (Table 1); previous estimate of conifer average is 56.3 m (Table 1)

height roses that Eq. 3 is sensitive to variations in canopy structure around the tower. For example, a pocket of increased canopy height corresponds to an area dominated by taller pines to the north-east of the tower. Probability distributions of daily average canopy height calculated during 2009 are compared to lidar statistics for each Cartesian quadrant in Fig. 8. Our average calculations in all quadrants are within one standard deviation of the lidar average heights, but there are clear differences between the distributions of lidar and calculated height (Fig. 8). In quadrant I, for example, we see taller heights expected in the region of tall pines, but the distribution does not capture the full range of heights seen with lidar. In quadrant IV, there is a general overestimation of the canopy height by Eq. 3.

### 3.5 Summary of Forest Canopy Results

Canopy heights, both calculated and reference, for the citrus grove, broadleaf, conifer and oak-savannah sites are compared in Fig. 9. We use the 2010 median calculation for the orchard, multi-year averages (see Table 4) for the evergreens and the four-quadrant average at the oak savannah. This allows us to see the results across multiple sites with different canopy

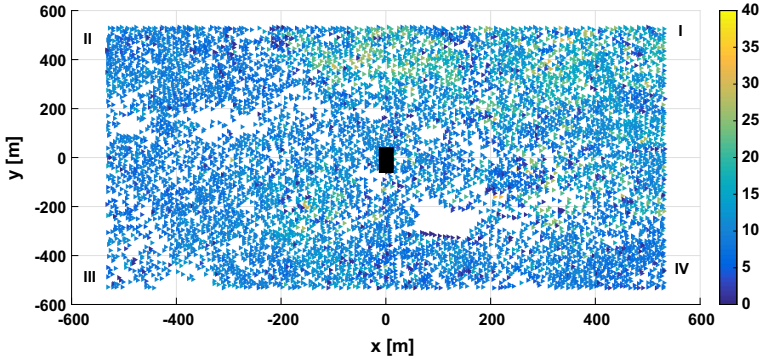


**Fig. 6** Tree height derived from lidar measurements around oak-savannah tower, located at (0,0) and marked by the black rectangle. The colour bar shows tree height in metres. Quadrants marked in roman numerals

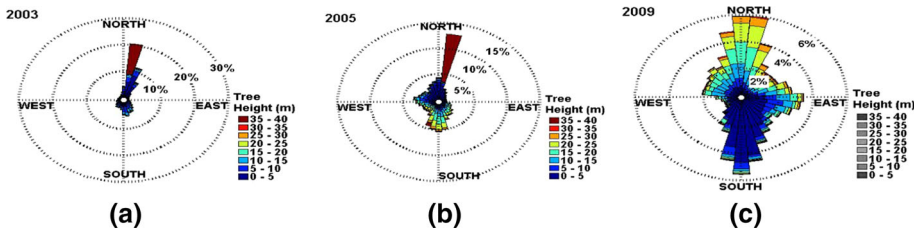


**Fig. 7** Height roses show distribution of calculated heights for three representative years (a, b, c) as a function of wind direction around the tower

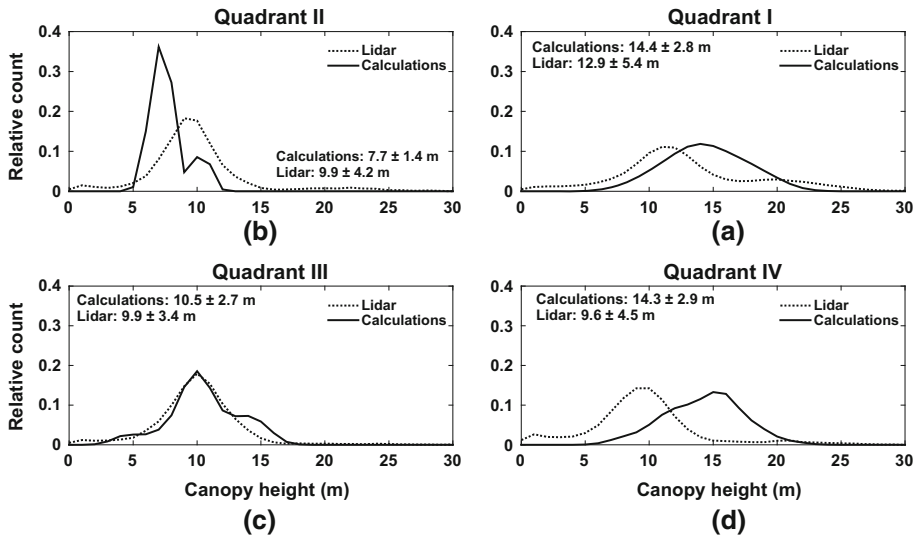


**Fig. 8** Distributions of canopy height from the lidar snapshot in 2009 and the calculated daily-averaged canopy heights in 2009. Each panel represents a different Cartesian quadrant (I–IV), (a)–(d) respectively. Averages for all distributions are shown with  $\pm 1$  SD

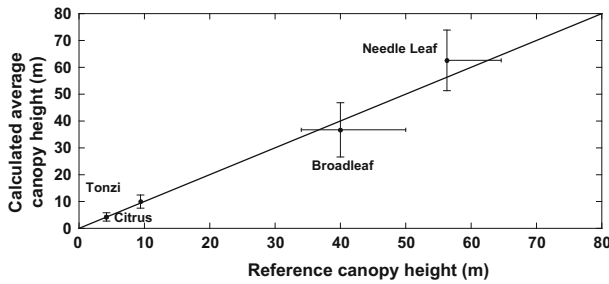


**Fig. 9** Comparison of calculated averages to reference values at four non-seasonal sites. *Vertical error bars* show one standard deviation around our calculations. *Horizontal error bars* show approximate range taken by lidar around average reference measurements (see Sect. 2.3). One-to-one line is shown for reference

structures in one place. Again, we include vertical error bars representing one standard deviation around average calculations and horizontal error bars for the uncertainty in our reference measurement (see Sect. 2.4). The value of *MAE* for the calculations compared to the one-to-one line is 2.6 while *MBE* =  $-0.9$ , indicating these results tend to be slightly higher than previous estimates on average.

## 4 Discussion

### 4.1 Accuracy, Precision and Applications

For the crop sites, our calculations successfully reproduce abrupt changes in canopy height caused by seasonal field maintenance and the growing season. Both the rice and alfalfa sites have roughly the same distributions of friction velocity and seem to experience the same average wind conditions. Furthermore, Fig. 1a shows that the anomalously high rice height (e.g., 4 m) does not correspond to  $u_*$  values outside the thresholds we set to remove the influence of extreme conditions. Figure 1b does not reveal any anomalous  $(u/u_*)^2$  values either. Since these data are already filtered by both friction velocity and stability, there does not appear to be any obvious physical justification for removing them. However, it is worth noting that Eq. 3 still captures a robust signal of seasonal growth with the rice over many years, despite the outliers. We see both positive and negative bias errors for a one-to-one model, indicating Eq. 3 does not consistently overestimate or underestimate canopy height. In the heterogeneous canopy, our method reproduces the quadrant distributions and statistics seen in lidar snapshots with mixed success. The calculated statistics are in reasonable agreement with the lidar statistics in all quadrants, but differences in the shapes of the height distributions (Fig. 8) are clear. A rough calculation using a two-dimensional footprint model (Hsieh et al. 2000) and average 2009 data reveals the average footprint of the tower to be about 400 m. Along with the fact that the average wind direction is approximately northerly to north-easterly (Fig. 7), this suggests the tower may not be sampling the same distribution of trees as the lidar instrument, especially in quadrants with larger discrepancies in height distribution shape. However, averaging all four quadrants together yields statistics consistent with the lidar measurements (Fig. 9). All of this indicates that using daily averages of Eq. 3 for estimating canopy height is generally accurate. Figures 3 and 9 also suggest that the precision indicated by the error bars is low, especially in the tall forest canopies. However, accounting

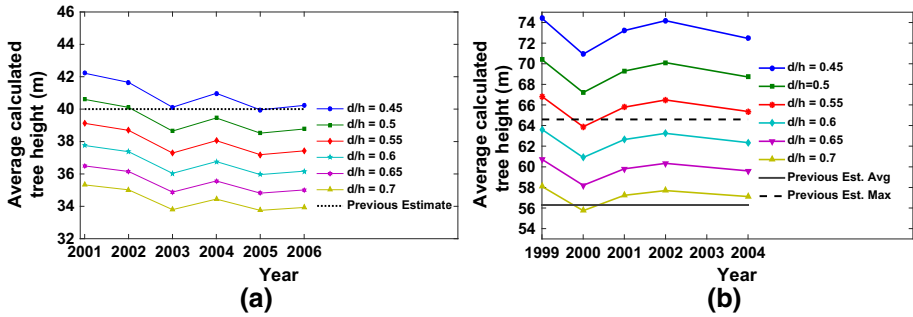


**Fig. 10** Sensitivity of yearly-average canopy height to varying  $d/h$  parameter at **a** broadleaf forest site and **b** conifer site. Results for  $z_0/h$  included in text

for imprecision in the validation averages, our calculations are in good agreement with all prior canopy height estimates over a range of canopy types (Fig. 9).

Phenology determined from continuous calculations of crop height can be used as an independent validation of model calculations of seasonal growth rate, maximum vegetation height and the timing of growth cycles (Osborne et al. 2007; Devkota et al. 2013). Furthermore, Timm et al. (2014) found that canopy height, along with LAI, can be used as a proxy for evapotranspiration from rice fields through the Penman–Monteith equation (Allen 1986). Because our method is sensitive to abrupt changes in crop height and can provide a continuous, accurate record without the need for field campaigns, calculated estimates should be considered in the context of energy and water balances to provide insight into crop-climate interactions.

The non-seasonal and forest site averages, which we show to be consistent over multiple years, can be independent metrics used for lidar validation. Lidar campaigns often use FLUXNET sites for validation points because of their global coverage and biome diversity (Simard et al. 2011), making it practical to apply our method as part of the verification process. We show that our calculations are already well within (Fig. 9) the range of lidar-estimated canopy heights at the broadleaf evergreen site (Hopkinson et al. 2013).

## 4.2 Next Steps

This study is intended to provide a first glimpse into the strengths and uncertainties of a routine technique for estimating canopy height using flux-tower data. We began with a series of assumptions about the utility of data from flux towers and canopy micrometeorology that have important implications for the accuracy of our canopy-height calculations. Addressing the error and uncertainty associated with each of these assumptions is necessary for improving the utility of Eq. 3 as a viable tool for estimating canopy height.

### 4.2.1 Eddy-Covariance Error

Measurements from sonic anemometers are the observational foundation of the eddy-covariance technique and are subject to instrumental error. For example, the design and positioning of sonic anemometer instrumentation has been found to force corrections to wind-speed measurements of  $-5$  to  $37\%$ , resulting in flux errors of about  $11\%$  (Kochendorfer et al. 2012), though further work showed errors of this magnitude to be less likely (Mauder 2013). A variety of methods have been proposed based on analysis of FLUXNET

time series to identify these and other sources of error (Hollinger and Richardson 2005). Researchers at many flux sites have sought to minimize so-called ‘transducer-shadow’ and ‘angle-of-attack’ effects based on other work (Gash and Dolman 2003). Low wind speeds and damped turbulent mixing are known to negatively bias flux measurements and increase the spread associated with meteorological measurements (Dyer and Hicks 1972; Gu et al. 2005). Because we consider data from only near-neutral conditions, we avoid the problem of flux underestimation in a stable nocturnal boundary layer. Our friction velocity filtering further ensures that there are sufficiently high turbulence levels for eddy-covariance measurements to be considered robust (Papale et al. 2006) and that the sampled canopy is not significantly deformed by high wind stress. Further improvements to the design of eddy-covariance towers and advances in the ability to filter erroneous flux data will strengthen the implementation of flux-tower data for estimating canopy height.

#### 4.2.2 Parametrization Error

Equation 3 is also sensitive to the assumption of simple relationships between canopy height and zero plane displacement and roughness length, respectively. These parametrizations are functions of LAI, an important site variable often measured at flux towers (Raupach 1994). LAI varies widely both in space and time, particularly in tall forests that undergo ecological change (Aber 1979; Parker et al. 2004). In Fig. 10 we show the results of simple sensitivity tests to determine what range of canopy heights would be obtained from varying  $d/h$  and  $z_0/h$  at the broadleaf (Tumbarumba) and conifer (Wind River) sites.

These initial sensitivity tests reveal that yearly average canopy heights at both the broadleaf and conifer can change significantly depending on the choice of  $d/h$ ;  $z_0/h$  also varies by about 50 % with a range of  $z_0/h$  ratios from 0.05 to 0.2. Further analysis is needed, especially at forest sites subject to ecological variability, to determine the appropriate values of  $d/h$  and  $z_0/h$  for use in Eq. 3. Recent work has made it possible to estimate roughness length and zero-plane displacement from space, opening up the possibility of validating our choice using external measurements (Tian et al. 2011).

#### 4.2.3 Tower Footprint

One of the strengths of our method is the ability to sample variability in heterogeneous canopy structure around a tower using wind direction. At the oak-savannah site (Tonzi) we use airborne lidar as validation, and we propose using our technique for lidar verification. Both tower measurements (Kim et al. 2006; Chen et al. 2009) and lidar (Dubayah and Drake 2000; Drake et al. 2002) are only valid over a certain footprint that affects interpretation of any results. Understanding the tower footprint can be challenging (Finnigan 2004), but models such as the one used here for a rough estimate at the oak savannah (Hsieh et al. 2000) can provide useful insight. Future work will focus on calculating a footprint-weighted canopy height to ensure that any comparisons to lidar use consistent footprints.

#### 4.2.4 The Roughness Sublayer

At the citrus grove site, Eq. 3 is applied to measurements taken at two different tower heights. One of the tower heights (7.11 m) was likely within the roughness sublayer because it was at less than twice the canopy height, while the other (9.18 m) was above the  $2h$  threshold. Average canopy heights from both tower heights are roughly the same, but the median height

calculated from the 9.18-m level is in better agreement with the previous estimates of Fares et al. (2012). Perhaps unsurprisingly, this indicates our method provides the best results when using wind and turbulence measurements taken at heights where Monin–Obukhov similarity theory is robust. Sites with tower instruments firmly within  $2h$  are likely poor choices for future applications. New theories for wind profiles very close to the canopy could improve the viability of our approach at these sites (Harman and Finnigan 2007).

#### 4.2.5 Choice of $z/L$ Threshold

Excluding data using a  $|z/L|$  threshold has important ramifications for estimating canopy height with our method because of the impact of non-neutral conditions on the logarithmic profile. At our sites, the choice of  $|z/L|$  filter has a larger impact on sample size, and thus sampling error in our calculations (Moncrieff et al. 1996; Hollinger and Richardson 2005), than it does on deviations from an exact logarithmic profile as determined by  $\phi_M$ . The development of a quantitative and site-specific methodology for determining near-neutral  $|z/L|$  thresholds that maintains an appropriate amount of data with which to calculate both daily and yearly averages should guide future analysis.

## 5 Conclusions

Using surface-layer theory and observations of wind speed made when  $|z/L| < 0.1$ , and within a set range of friction velocities, we have calculated average vegetation height in short, intermediate and tall canopies with validation by field measurements and lidar. Daily-averaged height calculations capture seasonal crop development at both rice and alfalfa sites, while yearly and multi-year averages are most reliable at intermediate and tall forest sites. At the heterogeneous oak savannah, differences in tower and lidar footprint likely contribute to more variability in the agreement of calculated heights with lidar references on a quadrant-by-quadrant basis. Overall site statistics are still robust, however. All of the calculations from these preliminary, but diverse, case studies show that our method provides accurate but imprecise daily heights in crops and yearly and multi-year averages at forest sites. Future investigations will focus on the development of site-specific filtering criteria and values of  $d/h$  and  $z_0/h$  to improve calculation accuracy and precision.

**Acknowledgments** We acknowledge the following AmeriFlux sites for their data records: US-Ton, US-Var, US-Tw3, US-Twt, US-Wrc and US-Lin. In addition, funding for AmeriFlux data resources was provided by the U.S. Department of Energy's Office of Science. Funding for AmeriFlux core site data, US-Ton, US-Var, US-Tw3, US-Twt, was provided by the U.S. Department of Energy's Office of Science, the USDA-AFRI project and the California Department of Water Resources. We acknowledge the FLUXNET project and OZFLUX for providing data from the Australian site, AU-Tum. In addition, we thank Silvano Fares and Allen Goldstein for providing their citrus grove data and for insightful discussions about the analysis. We appreciate the helpful comments of the anonymous reviewers and Berkeley Biometeorology Lab members Cove Sturtevant and Sara Knox that greatly improved the manuscript. Thank you to Joe Verfaillie for maintaining the rice, alfalfa and tonzi site equipment and data.

## References

Aber JD (1979) Foliage-height profiles and succession in northern hardwood forests. *Ecology* 60:18–23. doi:10.2307/1936462

- Allen RG (1986) A Penman for all seasons. *J Irrig Drain Eng* 112:348–368. doi:[10.1061/\(ASCE\)0733-9437\(1986\)112:4\(348\)](https://doi.org/10.1061/(ASCE)0733-9437(1986)112:4(348))
- Baldocchi DD, Chen Q, Chen X, et al (2010) The dynamics of energy, water, and carbon fluxes in a blue oak (*Quercus douglasii*) savanna in California. In: Hill M, Hanan N (eds) *Ecosystem Function in Savannas*, Taylor and Francis Group, Boca Raton, FL, p 135–154
- Chen B, Black TA, Coops NC et al (2009) Assessing tower flux footprint climatology and scaling between remotely sensed and eddy covariance measurements. *Boundary-Layer Meteorol* 130:137–167. doi:[10.1007/s10546-008-9339-1](https://doi.org/10.1007/s10546-008-9339-1)
- Chen G, Hay GJ (2011) An airborne lidar sampling strategy to model forest canopy height from Quickbird imagery and GEOBIA. *Remote Sens Environ* 115:1532–1542. doi:[10.1016/j.rse.2011.02.012](https://doi.org/10.1016/j.rse.2011.02.012)
- Chen Q, Baldocchi D, Gong P, Kelly M (2006) Isolating individual trees in a savanna woodland using small footprint lidar data. *Photogramm Eng Remote Sens* 72:923–932
- Devkota KP, Manschadi AM, Devkota M et al (2013) Simulating the impact of climate change on rice phenology and grain yield in irrigated drylands of Central Asia. *J Appl Meteorol Climatol* 52:2033–2050. doi:[10.1175/JAMC-D-12-0182.1](https://doi.org/10.1175/JAMC-D-12-0182.1)
- Dickinson RE, Hanson B (1984) Vegetation-albedo feedbacks. In: Hansen J, Takahashi T (eds) *Climate Processes and Climate Sensitivity*, American Geophysical Union, Washington, DC, p 180–186
- Drake JB, Dubayah RO, Knox RG et al (2002) Sensitivity of large-footprint lidar to canopy structure and biomass in a neotropical rainforest. *Remote Sens Environ* 81:378–392. doi:[10.1016/S0034-4257\(02\)00013-5](https://doi.org/10.1016/S0034-4257(02)00013-5)
- Drake JB, Knox RG, Dubayah RO et al (2003) Above-ground biomass estimation in closed canopy Neotropical forests using lidar remote sensing: factors affecting the generality of relationships. *Glob Ecol Biogeogr* 12:147–159. doi:[10.1046/j.1466-822X.2003.00010.x](https://doi.org/10.1046/j.1466-822X.2003.00010.x)
- Draxl C, Hahmann A, Pena A, Giebel G (2012) Evaluating winds and vertical wind shear from Weather Research and Forecasting model forecasts using seven planetary boundary layer schemes. *Wind Energy* 17:39–55. doi:[10.1002/we](https://doi.org/10.1002/we)
- Dubayah RO, Drake JB (2000) Lidar remote sensing for forestry applications. *J For* 98:44–46
- Dyer AJ (1974) A review of flux-profile relationships. *Boundary-Layer Meteorol* 7:363–372. doi:[10.1007/BF00240838](https://doi.org/10.1007/BF00240838)
- Dyer AJ, Hicks BB (1972) The spatial variability of eddy fluxes in the constant flux layer. *Q J R Meteorol Soc* 98:206–212. doi:[10.1002/qj.49709841518](https://doi.org/10.1002/qj.49709841518)
- Fares S, Weber R, Park JH et al (2012) Ozone deposition to an orange orchard: partitioning between stomatal and non-stomatal sinks. *Environ Pollut* 169:258–266. doi:[10.1016/j.envpol.2012.01.030](https://doi.org/10.1016/j.envpol.2012.01.030)
- Finnigan J (2004) The footprint concept in complex terrain. *Agric For Meteorol* 127:117–129. doi:[10.1016/j.agrformet.2004.07.008](https://doi.org/10.1016/j.agrformet.2004.07.008)
- Finnigan JJ (1979) Turbulence in waving wheat. *Boundary-Layer Meteorol* 16:181–211
- Finnigan JJ (2000) Turbulence in plant canopies. *Annu Rev Fluid Mech* 32(519):571. doi:[10.2480/agrmet.20.1](https://doi.org/10.2480/agrmet.20.1)
- Gardiner BA (1994) Wind and wind forces in a plantation spruce forest. *Boundary-Layer Meteorol* 67:161–186. doi:[10.1007/BF00705512](https://doi.org/10.1007/BF00705512)
- Garratt JR (1994) *The atmospheric boundary layer*. Cambridge University Press, Cambridge, 316 pp
- Gash JHC, Dolman AJ (2003) Sonic anemometer (co)sine response and flux measurement: I. The potential for (co)sine error to affect sonic anemometer-based flux measurements. *Agric For Meteorol* 119:195–207. doi:[10.1016/S0168-1923\(03\)00137-0](https://doi.org/10.1016/S0168-1923(03)00137-0)
- Gu L, Falge EM, Boden T et al (2005) Objective threshold determination for nighttime eddy flux filtering. *Agric For Meteorol* 128:179–197. doi:[10.1016/j.agrformet.2004.11.006](https://doi.org/10.1016/j.agrformet.2004.11.006)
- Harman IN, Finnigan JJ (2007) A simple unified theory for flow in the canopy and roughness sublayer. *Boundary-Layer Meteorol* 123:339–363. doi:[10.1007/s10546-006-9145-6](https://doi.org/10.1007/s10546-006-9145-6)
- Hogstrom U (1988) Non-dimensional wind and temperature profiles in the atmospheric surface layer: a re-evaluation. *Boundary-Layer Meteorol* 42:55–78. doi:[10.1007/BF00119875](https://doi.org/10.1007/BF00119875)
- Hollinger DY, Richardson A D (2005) Uncertainty in eddy covariance measurements and its application to physiological models. *Tree Physiol* 25:873–885. doi:[10.1093/treephys/25.7.873](https://doi.org/10.1093/treephys/25.7.873)
- Hopkinson C, Lovell J, Chasmer L et al (2013) Integrating terrestrial and airborne lidar to calibrate a 3D canopy model of effective leaf area index. *Remote Sens Environ* 136:301–314. doi:[10.1016/j.rse.2013.05.012](https://doi.org/10.1016/j.rse.2013.05.012)
- Hsieh CI, Katul G, Chi TW (2000) An approximate analytical model for footprint estimation of scalar fluxes in thermally stratified atmospheric flows. *Adv Water Resour* 23:765–772. doi:[10.1016/S0309-1708\(99\)00042-1](https://doi.org/10.1016/S0309-1708(99)00042-1)
- Kane VR, McGaughey RJ, Bakker JD et al (2010) Comparisons between field- and LiDAR-based measures of stand structural complexity. *Can J For Res* 40:761–773. doi:[10.1139/X10-024](https://doi.org/10.1139/X10-024)



- Kim J, Guo Q, Baldocchi DD et al (2006) Upscaling fluxes from tower to landscape: overlaying flux footprints on high-resolution (IKONOS) images of vegetation cover. *Agric For Meteorol* 136:132–146. doi:[10.1016/j.agrformet.2004.11.015](https://doi.org/10.1016/j.agrformet.2004.11.015)
- Knox SH, Sturtevant C, Matthes JH et al (2014) Agricultural peatland restoration: effects of land-use change on greenhouse gas (CO<sub>2</sub> and CH<sub>4</sub>) fluxes in the Sacramento–San Joaquin Delta. *Glob Change Biol*. doi:[10.1111/gcb.12745](https://doi.org/10.1111/gcb.12745)
- Kochendorfer J, Meyers T, Frank J et al (2012) How well can we measure the vertical wind speed? Implications for fluxes of energy and mass. *Boundary-Layer Meteorol* 145:383–398. doi:[10.1007/s10546-012-9738-1](https://doi.org/10.1007/s10546-012-9738-1)
- Lefsky MA, Cohen WB, Harding DJ et al (2002) Lidar remote sensing of above-ground biomass in three biomes. *Glob Ecol Biogeogr* 11:393–399. doi:[10.1046/j.1466-822x.2002.00303.x](https://doi.org/10.1046/j.1466-822x.2002.00303.x)
- Lefsky MA, Harding DJ, Keller M et al (2005) Estimates of forest canopy height and aboveground biomass using ICESat. *Geophys Res Lett* 32:L22S02. doi:[10.1029/2005GL023971](https://doi.org/10.1029/2005GL023971)
- Leuning R, Cleugh HA, Zegelin SJ, Hughes D (2005) Carbon and water fluxes over a temperate Eucalyptus forest and a tropical wet/dry savanna in Australia: measurements and comparison with MODIS remote sensing estimates. *Agric For Meteorol* 129:151–173. doi:[10.1016/j.agrformet.2004.12.004](https://doi.org/10.1016/j.agrformet.2004.12.004)
- Lovell JL, Jupp DLB, Culvenor DS, Coops NC (2003) Using airborne and ground-based ranging lidar to measure canopy structure in Australian forests. *Can J Remote Sens* 29:607–622. doi:[10.5589/m03-026](https://doi.org/10.5589/m03-026)
- Ma S, Baldocchi DD, Xu L, Hehn T (2007) Inter-annual variability in carbon dioxide exchange of an oak/grass savanna and open grassland in California. *Agric For Meteorol* 147:157–171. doi:[10.1016/j.agrformet.2007.07.008](https://doi.org/10.1016/j.agrformet.2007.07.008)
- Marcolla B, Cescatti A, Montagnani L et al (2005) Importance of advection in the atmospheric CO<sub>2</sub> exchanges of an alpine forest. *Agric For Meteorol* 130:193–206. doi:[10.1016/j.agrformet.2005.03.006](https://doi.org/10.1016/j.agrformet.2005.03.006)
- Mascaro J, Detto M, Asner GP, Muller-Landau HC (2011) Evaluating uncertainty in mapping forest carbon with airborne LiDAR. *Remote Sens Environ* 115:3770–3774. doi:[10.1016/j.rse.2011.07.019](https://doi.org/10.1016/j.rse.2011.07.019)
- Mauder M (2013) A comment on how well can we measure the vertical wind speed? Implications for fluxes of energy and mass by Kochendorfer et al. *Boundary-Layer Meteorol* 147:329–335. doi:[10.1007/s10546-012-9794-6](https://doi.org/10.1007/s10546-012-9794-6)
- Metzger M, McKeon BJ, Holmes H (2007) The near-neutral atmospheric surface layer: turbulence and non-stationarity. *Philos Trans A Math Phys Eng Sci* 365:859–876. doi:[10.1098/rsta.2006.1946](https://doi.org/10.1098/rsta.2006.1946)
- Moncrieff JB, Malhi Y, Leuning R (1996) The propagation of errors in long-term measurements of land-atmosphere fluxes of carbon and water. *Glob Change Biol* 2:231–240. doi:[10.1111/j.1365-2486.1996.tb00075.x](https://doi.org/10.1111/j.1365-2486.1996.tb00075.x)
- Ni W, Woodcock CE (2000) Effect of canopy structure and the presence of snow on the albedo of boreal conifer forests. *J Geophys Res Atmos* 105:11879–11888. doi:[10.1029/1999JD901158](https://doi.org/10.1029/1999JD901158)
- Oncley S, Friehe C, Larue J et al (1996) Surface-layer fluxes, profiles, and turbulence measurements over uniform terrain under near-neutral conditions. *J Atmos Sci* 53:1029–1044
- Osborne TM, Lawrence DM, Challinor AJ et al (2007) Development and assessment of a coupled crop-climate model. *Glob Change Biol* 13:169–183. doi:[10.1111/j.1365-2486.2006.01274.x](https://doi.org/10.1111/j.1365-2486.2006.01274.x)
- Papale D, Reichstein M, Aubinet M et al (2006) Towards a standardized processing of Net Ecosystem Exchange measured with eddy covariance technique: algorithms and uncertainty estimation. *Biogeosciences* 3:571–583. doi:[10.5194/bg-3-571-2006](https://doi.org/10.5194/bg-3-571-2006)
- Parker GG, Harmon ME, Lefsky MA et al (2004) Three-dimensional structure of an old-growth Pseudotsuga-Tsuga canopy and its implications for radiation balance, microclimate, and gas exchange. *Ecosystems* 7:440–453. doi:[10.1007/s10021-004-0136-5](https://doi.org/10.1007/s10021-004-0136-5)
- Paw UKT, Falk M, Suchanek TH et al (2004) Carbon dioxide exchange between an old-growth forest and the atmosphere. *Ecosystems* 7:513–524
- Peña A, Floors R, Gryning SE (2014) The Høvsøre tall wind-profile experiment: a description of wind profile observations in the atmospheric boundary layer. *Boundary-Layer Meteorol* 150:69–89. doi:[10.1007/s10546-013-9856-4](https://doi.org/10.1007/s10546-013-9856-4)
- Raupach MR (1994) Simplified expressions for vegetation roughness length and zero-plane displacement as functions of canopy height and area index. *Boundary-Layer Meteorol* 71:211–216. doi:[10.1007/BF00709229](https://doi.org/10.1007/BF00709229)
- Raupach MR, Finnigan JJ, Brunei Y (1996) Coherent eddies and turbulence in vegetation canopies: the mixing-layer analogy. *Boundary-Layer Meteorol* 78:351–382. doi:[10.1007/BF00120941](https://doi.org/10.1007/BF00120941)
- Saremi H, Kumar L, Turner R, Stone C (2014) Airborne LiDAR derived canopy height model reveals a significant difference in radiata pine (*Pinus radiata* D. Don) heights based on slope and aspect of sites. *Trees-Struct Funct* 28:733–744. doi:[10.1007/s00468-014-0985-2](https://doi.org/10.1007/s00468-014-0985-2)
- Shaw RH, Pereira a (1982) Aerodynamic roughness of a plant canopy: a numerical experiment. *Agric Meteorol* 26:51–65. doi:[10.1016/0002-1571\(82\)90057-7](https://doi.org/10.1016/0002-1571(82)90057-7)

- Simard M, Pinto N, Fisher JB, Baccini A (2011) Mapping forest canopy height globally with spaceborne lidar. *J Geophys Res* 116:G04021. doi:[10.1029/2011JG001708](https://doi.org/10.1029/2011JG001708)
- Thomas RQ, Hurtt GC, Dubayah R, Schilz MH (2008) Using lidar data and a height-structured ecosystem model to estimate forest carbon stocks and fluxes over mountainous terrain. *Can J Remote Sens* 34:S351–S363. doi:[10.5589/m08-036](https://doi.org/10.5589/m08-036)
- Tian X, Li ZY, Van der Tol C et al (2011) Estimating zero-plane displacement height and aerodynamic roughness length using synthesis of LiDAR and SPOT-5 data. *Remote Sens Environ* 115:2330–2341
- Timm AU, Roberti DR, Streck NA et al (2014) Energy partitioning and evapotranspiration over a rice paddy in Southern Brazil. *J Hydrometeorol* 15:1975–1988. doi:[10.1175/JHM-D-13-0156.1](https://doi.org/10.1175/JHM-D-13-0156.1)
- Willmott CJ, Matsuura K (2005) Advantages of the mean absolute error (MAE) over the root mean square error (RMSE) in assessing average model performance. *Clim Res* 30:79–82. doi:[10.3354/cr030079](https://doi.org/10.3354/cr030079)